Interpreting ultrafast molecular fragmentation dynamics with *ab initio* electronic structure calculations

Carlos Trallero,[1] Brett J. Pearson,[2] Thomas Weinacht,[3,a)] Kandis Gilliard,[4] and Spiridoula Matsika[4,b)]
[1]*Staecie Institute for Molecular Sciences, Ottawa, Ontario K1A 0R6, Canada*
[2]*Department of Physics and Astronomy, Dickinson College, Carlisle, Pennsylvania 17013, USA*
[3]*Department of Physics and Astronomy, Stony Brook University, Stony Brook, New York 11794, USA*
[4]*Department of Chemistry, Temple University, Philadelphia, Pennsylvania 19122, USA*

(Received 19 December 2007; accepted 23 January 2008; published online 26 March 2008)

High-level *ab initio* electronic structure calculations are used to interpret the fragmentation dynamics of $CHBr_2COCF_3$, following excitation with an intense ultrafast laser pulse. The potential energy surfaces of the ground and excited cationic states along the dissociative $C-CF_3$ bond have been calculated using multireference second order perturbation theory methods. The calculations confirm the existence of a charge transfer resonance during the evolution of a dissociative wave packet on the ground state potential energy surface of the molecular cation and yield a detailed picture of the dissociation dynamics observed in earlier work. Comparisons of the ionic spectrum for two similar molecules support a general picture in which molecules are influenced by dynamic resonances in the cation during dissociation. © *2008 American Institute of Physics*.
[DOI: 10.1063/1.2850524]

I. INTRODUCTION

Molecular ionization by a strong field, ultrafast laser pulse is typically accompanied by wave packet motion on ionic potential energy surfaces (PES) of the molecule since the equilibrium configuration of the ion generally differs from that of the neutral. These wave packet dynamics in the ionic PES can have a significant effect on the fragmentation of the molecule, particularly if there are low-lying ionic states that are accessible from the ground state of the ion with a subsequent laser pulse (via single-photon absorption in the visible or near infrared region 1.5–3 eV). The importance of ionic resonances has been debated in the literature,[1–4] with recent work highlighting the importance of wave packet motion across resonances in determining molecular fragmentation patterns.[5,6]

While experimental work has made a strong case for the role of ionic resonances in molecular fragmentation with intense ultrafast laser pulses, there has been less detailed theoretical work to support the interpretation of these experiments, and it has therefore been difficult to interpret measured quantities in terms of time-dependent structures such as bond lengths and angles as a function of time for a given set of electronic states. Here, we show how combining pump-probe measurements of fragment ion yields with *ab initio* electronic structure calculations can yield a detailed picture of the fragmentation dynamics. We are interested in gaining both a detailed quantitative picture of the fragmentation in a particular system, as well as a qualitative picture of trends among families of similar molecules. We performed calculations for the ionic states of $CHBr_2COCF_3^+$ and compared our results with calculations for $CH_3COCF_3^+$. The results support our interpretation of the dynamics in $CHBr_2COCF_3$ and point toward a general criterion for determining when ionic resonances should play an important role in ultrafast molecular fragmentation.

II. EXPERIMENTAL APPARATUS

Since the focus of this work is computational, we provide only a brief description of the experimental apparatus (described in detail elsewhere[7]). We use a Ti:sapphire laser system that produces 30 fs laser pulses with 1 mJ of energy at a repetition rate of 1 kHz. The pulses are directed into a Mach–Zehnder interferometer, where one arm contains an acousto-optic modulator based pulse shaper. The pulse shaper allows control over both the phase and amplitude of the pump pulses. The other arm of the interferometer acts as a variable delay for a second pulse used to probe the dynamics initiated by the pump laser pulse. The photon energy of both pump and probe laser pulses is 1.5 eV. The pulses are focused into an effusive molecular beam, and ions are collected in a time-of-flight mass spectrometer (TOFMS). Peak laser intensities in the interaction region reach the low 10^{14} W/cm^2. In order to control the ratio of molecular fragments, we use a genetic algorithm to design optimal laser pulse shapes based on the fragment ion yields in the TOFMS.

III. THEORETICAL METHODS

Initially, the ground state of neutral $CHBr_2COCF_3$ and its cation were optimized at the MP2 level of theory using the Dunning correlation consistent double zeta (cc-PVDZ) basis sets for all atoms.[8,9] Constrained minimizations for the ground cationic state were carried out where the $C-CF_3$

a)Electronic mail: thomas.weinacht@stonybrook.edu.
b)Author to whom correspondence should be addressed. smatsika@temple.edu.

bond was kept fixed and all other coordinates were relaxed. These optimizations were done at two different levels of theory. A set of geometries was obtained using unrestricted many-body perturbation theory (UMP2) and the Los Alamos effective core potentials (ECPs) on the Br atoms.[10] Tests showed that the ECPs do not have a significant effect on the geometries. Optimized structures were also obtained using the complete active space self–consistent field (CASSCF) method with all electrons on Br and cc-PVDZ basis sets on all atoms. The complete active space consisted of 13 electrons in 9 orbitals [denoted (13,9)]. The occupied orbitals at the equilibrium geometry are mainly four *p* orbitals localized on the Br atoms (lone pairs) and three orbitals on the carbonyl group. For each of the two sets of optimized geometries, the energies of the five lowest excited states were obtained using the multiconfigurational quasidegenerate second order perturbation theory (MCQDPT2) method, with orbitals from an average-of-states CASSCF(13,9). The PES calculated at the MCQDPT2 level using these two sets of geometries are almost parallel to each other, with the MCQDPT2 energies at the UMP2 geometries being lower by ~0.3 eV from the MCQDPT2 energies at the CASSCF geometries. Thus, the qualitative picture is similar for the two sets of results, but the UMP2 geometries are closer to the actual minimum energy path at the MCQDPT2 level, so only the UMP2 results are shown in the following discussions.

The effect of spin-orbit coupling was calculated at the equilibrium geometry of $CHBr_2COCF_3^+$ using the CASSCF wave functions and the Breit–Pauli spin-orbit operator with full one electron contributions but only the core-active two electron contributions as implemented in GAMESS.[11]

PES were also calculated for $CH_3COCF_3^+$. Constrained minimizations were carried out for the ground cationic state where the $C-CF_3$ bond was kept fixed and all other coordinates were relaxed. The main objective for studying this system was to obtain the excited state energies of the CH_3COCF_3 cation, so only the UHF method with a cc-PVDZ for all atoms was used for the optimizations. CASSCF followed with MCQDPT2 was used to calculate the excited states of the cation along the dissociative curve. An active space of five electrons in five orbitals was used and three electronic states were included in the calculations.

Various fragments at the dissociation limits, such as $CHBr_2CO^+$, $CHBr_2CO$, CF_3, CF_3^+, CH_3CO^+, CH_3CO, CO, and $CHBr_2^+$ were optimized at the MP2/cc-PVDZ or UMP2/cc-PVDZ level for the radicals. The GAUSSIAN suite of programs[12] was used for some MP2 optimizations with ECPs and the GAMESS suite of programs[11] was used for all the other calculations.

IV. EXPERIMENTAL RESULTS

Figure 1 summarizes our experimental results, which have been published separately[13] but are included here for the convenience of the reader. The main figure shows the $CHBr_2^+$, $CHBr_2CO^+$, and CF_3^+ fragment yields as a function of pump-probe delay. These are the three main fragments in the TOFMS for pulses with peak intensities below 2×10^{14} W/cm^2. The inset shows the $CF_3^+/CHBr_2^+$ ratio for a pulse shaped to maximize or minimize this ratio in the TOFMS. The peak intensities of the pump and probe pulses for the pump-probe data are about 2×10^{14} and 3×10^{13} W/cm^2, respectively. The peak intensity of the pulse used for the control experiment is about 1×10^{14} W/cm^2 without pulse shaping. The optimal pulse shape for maximizing the $CF_3^+/CHBr_2^+$ ratio shown in the inset to the figure contained a double pulse structure with the pulse separation matching the time at which CF_3^+ undergoes a maximum in the pump-probe signal.[13]

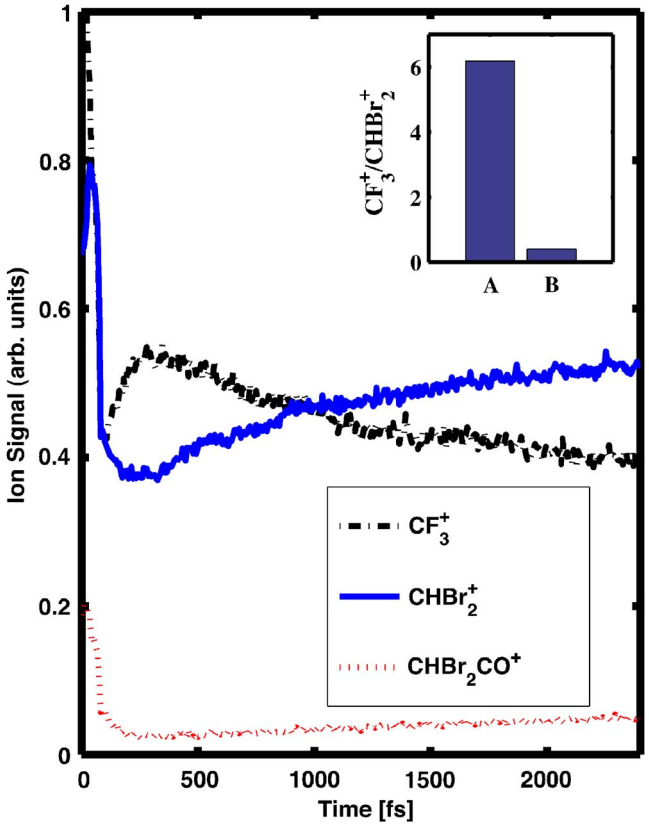

FIG. 1. (Color online) Fragment yields as a function of pump-probe delay. Inset: $CF_3^+/CHBr_2^+$ ratio for a pulse optimized to maximize (A) and minimize (B) this ratio.

V. THEORETICAL RESULTS

In the experiments, ionization of the molecule launches a vibrational wave packet on the ground ionic state PES (as well as possibly some excited ionic states). In order to understand the ensuing dynamics and how the wave packet interacts with the probe pulse to produce different ionic fragments, we calculated the lowest five electronic states of the ion as a function of the $C-CF_3$ bond length. We chose this as the dissociation coordinate since two of the three main fragments observed in the experiments, $CHBr_2CO^+$ and CF_3^+, indicate that this bond breaks following rapid ionization. Geometries along the dissociation path were obtained by constrained minimization with the $C-CF_3$ bond length fixed at each point. Figure 2 shows the ground state PES calculated at these geometries (using the MCQDPT2 method) plotted as a function of the $C-CF_3$ and $C-CHBr_2$ coordinates. At distances less than 1.9 Å, two different minima were obtained

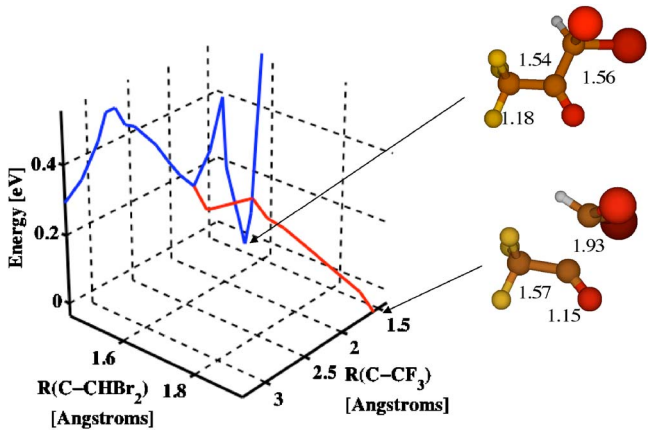

FIG. 2. (Color online) Potential energy surfaces of the ground ionic state of $CHBr_2COCF_3^+$ along the $CF_3-COCHBr_2$ and $CF_3CO-CHBr_2$ bonds. Note that there are two barriers along the $CF_3-COCHBr_2$ bond and one barrier along the $CF_3CO-CHBr_2$ bond. The molecular pictures indicate the geometries at the minimum along the $CF_3-COCHBr_2$ bond and at the far side of the barrier along the $CF_3CO-CHBr_2$ bond. The numbers beside the pictures indicate the C–C and C–O bond lengths in Å.

at a given $C-CF_3$ distance, corresponding to a branching of the PES, as shown in Fig. 2. Furthermore, two minima have been found for the cation even in optimizations without any constraint. One branch leads to a minimum denoted $D_0(m1)$ in which both C–C bonds are ~1.5 Å and the C–O bond is 1.18 Å. $D_0(m1)$ is found starting from the geometry of the neutral. The other branch stretches the $C-CHBr_2$ bond and leads to a minimum [denoted $D_0(m2)$] where the $C-CHBr_2$ bond is increased substantially to 1.9 Å. The two minima are almost isoenergetic at the MCQDPT2 level of theory. The first minimum $D_0(m1)$ is separated from direct dissociation by two barriers of ~0.5 eV each.

The excited states along the main dissociation path as a function of $C-CF_3$ distance are shown in Fig. 3. The five lowest ionic states obtained using MCQDPT2 theory at MP2 optimized geometries are shown. The dashed horizontal line in Fig. 3 corresponds to the energy of the ground state at the equilibrium position of the neutral molecule and, thus, the minimum possible energy of the wave packet upon ionization. The ground state minimum is separated from direct dissociation by barriers of ~0.5 eV, which is less than the initial energy of the wave packet. The four lowest excited states at the minimum are within 2 eV from the ground state, but they quickly rise in energy as the $C-CF_3$ bond length increases, while the ground state remains relatively flat. The two different dissociation channels are shown at the right of the figure. The ground state dissociates to $CHBr_2CO^+ + CF_3$, while the first excited state dissociates to $CHBr_2CO + CF_3^+$. An arrow at $R(C-CF_3)=1.85$ Å shows where the separation between the ground state D_0 and the first excited state D_1 is 1.5 eV. A charge transfer resonance can occur if a probe pulse arrives at this time.

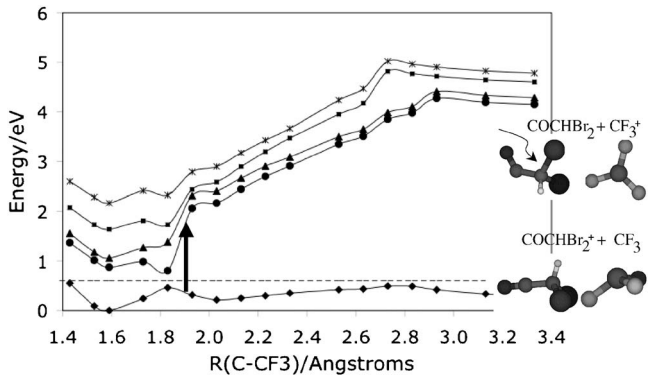

FIG. 3. Potential energy surfaces of the first five states of $CHBr_2COCF_3^+$ along the $CF_3-COCHBr_2$ bond. The dashed line correspond to the energy of the ion at vertical ionization. The structures shown correspond to the geometries of the fragments at complete dissociation and not at R(C–CF3)=3.35 Å. The length of the thick black arrow corresponds to the photon energy of the probe pulse.

It is worth commenting on the difficulties encountered in calculating accurate barriers to dissociation in these systems. Obtaining the PES along the C–C dissociation requires high-level calculations for both the optimizations and energies. At the uncorrelated UHF level, a barrier exists at approximately 2 Å. However, when dynamical correlation is used, the barrier may change dramatically. Previous work has shown that high-level correlated methods are needed to predict the barriers for dissociation in substituted acetone cations.[14] For example, in $CH_3COCF_3^+$ UHF gives a barrier of 0.5 eV, while CBS-QB3 reduces it to 0.027 eV.[14] In $CHBr_2COCF_3^+$, the situation becomes even more complicated because many states are close together energetically at initial ionization, and they can couple or switch order depending on the level of theory used. Thus, for $CHBr_2COCF_3^+$, both dynamical and nondynamical correlations are essential at all geometries, and a multiconfiguration self-consistent-field (MCSCF) wave function is needed to account for the multiconfigurational character even close to the minimum. As the bond begins to lengthen, a multiconfigurational wave function is needed to describe the bond breaking. Dynamical correlation is also essential to predict the correct energetics. The MCQDPT2 used here includes both dynamical and nondynamical correlations and describes the dissociative curve with good accuracy. A MCSCF method without dynamical correlation produced barriers that were too high.

As bromine has a large spin-orbit coupling, its effect was also tested in $CHBr_2COCF_3^+$ but was found to produce little change in the electronic energies of the cation at its equilibrium position. The effect on the first excited state was ~150 cm^{-1}, while for the higher excited states it was between 2 and 390 cm^{-1}.

VI. DISCUSSION

Vertical ionization of $CHBr_2COCF_3$ (where the geometry of the ion retains the equilibrium geometry of the neutral) leads to a ground ionic state that is almost degenerate with the first excited ionic state. Relaxation of the ground D_0 state leads to a minimum ~0.6 eV below vertical ionization, as shown in Fig. 3. The ground ionic state shows two barriers along the dissociation $C-CF_3$ pathway, with heights of 0.45 and 0.49 eV at the MCQDPT2 level of theory. Since these barriers are less than 0.6 eV, there is enough energy in the system to break the $C-CF_3$ bond (consistent with the experimental results).

TABLE I. Total energies (in hartrees) of various fragments involved in the dissociation of $CHBr_2COCF_3^+$ at the MP2/cc-pVDZ level of theory. The last column shows energy differences (ΔE) in eV.

Label	Fragment	Energy (hartrees)	ΔE (eV)
1^+	CF_3^+	−336.500 38	1^+-1: 8.43
1	CF_3	−336.810 28	
2^+	$COCHBr_2^+$	−5296.295 19	2^+-2: 7.07
2	$COCHBr_2$	−5296.554 87	
3^+	CF_3CO^+	−449.564 70	3^+-3: 7.89
3	CF_3CO	−449.854 53	
4^+	$CHBr_2^+$	−5183.227 36	4^+-4: 7.76
4	$CHBr_2$	−5183.512 61	
5^+	$COCH_3^+$	−152.511 44	5^+-5: 6.36
5	$COCH_3$	−152.745 22	
6	CO	−113.036 81	
7	$CF_3+COCHBr_2^+$	−5633.105 47	
8	$CF_3^++COCHBr_2$	−5633.055 25	8−7: 1.37
9	$CF_3CO+CHBr_2^+$	−5633.081 89	
10	$CF_3CO^++CHBr_2$	−5633.077 30	10−9: 0.12
11	$CF_3+COCH_3^+$	−489.321 72	
12	$CF_3^++COCH_3$	−489.245 60	12−11: 2.07
13	$CO+CHBr_2^+$	−5296.264 16	$13-2^+$: 0.84

After the first barrier, a branching occurs that leads to a separate minimum on the ionic state. This second minimum is almost isoenergetic with the first at the MCQDPT2 level of theory but has a distinct geometry. The main difference is a stretched $C-CHBr_2$ bond which indicates that it will likely break if branching occurs, leading to production of $CHBr_2^+$, one of the three main fragment ions measured in the TOFMS.

Dissociation of $CHBr_2COCF_3^+$ along the $C-CF_3$ bond leads to two possible dissociation channels: $CHBr_2CO^+ + CF_3$ and $CHBr_2CO+CF_3^+$. Table I shows the energies of these fragments (as well as others) calculated at the MP2 level of theory. The $CHBr_2CO^++CF_3$ channel is the lowest in energy and the $CHBr_2CO+CF_3^+$ channel is 1.37 eV higher. We note that the gap between the two channels shown in Fig. 3 is much higher, since this represents a vertical gap, while 1.37 eV is the adiabatic gap. The two values differ substantially because the relaxed geometries of the fragments for the excited channel, $CHBr_2CO+CF_3^+$, are very different from those of the ground state channel. Neutral CF_3 has a pyramidal structure with R(C–F)=1.32 Å, whereas the excited fragment CF_3^+ is planar with R(C–F)=1.24 Å. The ground state fragment $CHBr_2CO^+$ has a linear O–C–C angle with R(C–O)=1.14 Å, R(C–C)=1.46 Å, and R(C–Br)=1.94 Å. Neutral $CHBr_2CO$ has ∠C–C–O=129°, R(C–O)=1.18 Å, R(C–C)=1.53 Å, and R(C–Br)=1.95 Å. Thus, the C–C–O angle and the bond lengths differ substantially between the neutral and ionic fragments. These differences cause the vertical separation at the dissociation limit [~4 eV as R(C–CF3) approaches 3.3 Å in Fig. 3] to be much higher than the adiabatic one.

As mentioned above, our measurements indicate that the second C–C bond may also break and produce $CHBr_2^+$. One possibility is that this bond breaks after $CHBr_2CO^+$ is formed, in which case the sum of the energies of $CHBr_2^+ + CO$ is 0.84 eV above the energy of $CHBr_2CO^+$ at its equilibrium position. Alternatively, the bond could potentially break at any time along the $C-CF_3$ dissociation and therefore require less energy. For example, Fig. 2 indicates that after passing through the first barrier as $C-CF_3$ stretches, the $C-CHBr_2$ bond may break if the wave packet branches out along the path that leads to the elongated $C-CHBr_2$ bond. The two channels along this dissociation path are $CF_3CO + CHBr_2^+$ and $CF_3CO^++CHBr_2$. Table I shows that the first channel (leading to the formation of $CHBr_2^+$) is lower energetically, but only by 0.12 eV. We note that these are the final product energetics and do not encompass all the intermediates that may be involved during the dissociation.

The lowest two ionic potentials along the $C-CHBr_2$ and $C-CF_3$ bonds (see Fig. 2) predict the production of the three primary fragment ions we observe in our measurements: CF_3^+, $CHBr_2^+$, and $CHBr_2CO^+$. Since the barrier to dissociation along the $C-CF_3$ bond on the ground ionic state is smaller than the initial wave packet energy, the wave packet can proceed to dissociation resulting in both CF_3 and $CHBr_2CO^+$. Dissociation along the $C-CHBr_2$ bond, for which there is also a relatively small barrier, can produce $CHBr_2^+$. Excitation to the first excited ionic state during ionization of the molecule can lead to the production of CF_3^+ and $CHBr_2CO$.

At the vertical ionization position, there are four excited ionic states within 1 eV of the ground ionic state, with energies of 0.02, and 0.36, 0.49, and 1.02 eV above it. At the equilibrium geometry of the ion, these states are within 2.2 eV of the ground state (0.87, 1.06, 1.64, and 2.16 eV above it). The close proximity of ionic states suggests that more than one state may initially be populated, likely leading to different fragments. As the $C-CF_3$ bond stretches, the excited states increase their energy while the ground state remains relatively flat. The calculations show that a charge transfer resonance exists enroute to dissociation when the energy gap between the ground and first excited states of the ion passes through the photon energy of the probe pulse (~1.5 eV). This charge transfer resonance is predicted by the current calculations at approximately 1.9 Å for a vertical transition with the geometry of the excited state the same as the relaxed geometry of the ground state. The gap between the ground and excited states at the second minimum $[D_0(m2)]$ is also 1.5 eV, and absorption may occur at that geometry as well. Both of these resonances can lead to the production of CF_3^+, while suppressing the production of $CHBr_2$, as seen in both the pump-probe and control experiments for pulse separations of 200–300 fs.[13] Thus, our calculations support the interpretation of the pump-probe and control measurements[13] in terms of a charge transfer resonance between the ground and first excited states of the ion as the molecule moves toward dissociation, following ionization.

A final aim of this paper is to develop an understanding of why the electronic spectrum of $CHBr_2COCF_3^+$ has so many low-lying states and to consider which molecules we might expect to have a similar spectrum. Even at initial ionization of $CHBr_2COCF_3$, there are several closely spaced excited states of the formed ion. These states result from the fact that many different configurations exist for the unpaired

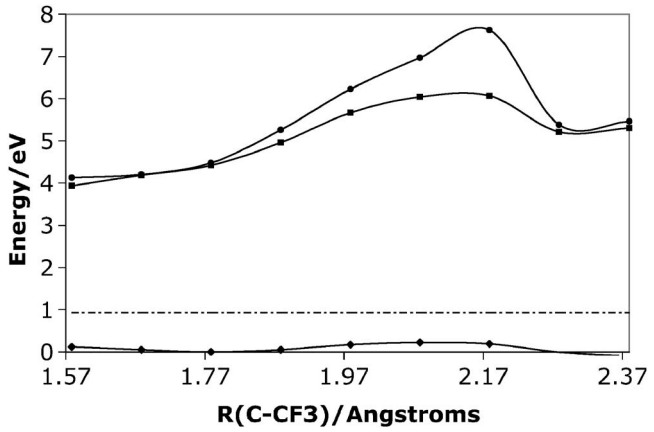

FIG. 4. Potential energy surfaces of the first three states of $CH_3COCF_3^+$ along the CF_3-COCH_3 bond. The dashed line corresponds to the energy of the ion at vertical ionization.

electron (or "hole") that is left after ionization. Specifically, we consider the energy required to remove an electron from either Br, F, or a carbonyl group when they are substituents to a methyl group. Ionization energies (IEs) for the halogenated methanes CH_3Br, CH_2Br_2, $CHBr_3$ are 10.24–10.6 eV, while the IE for CHF_3 and CH_3F are 13–14.8 eV. The IE of CH_2CO (formaldehyde) is 10.88 eV. These data show that the energy needed to remove an electron from Br or carbonyl attached to a methyl group is comparable but much less than that needed to remove an electron from F attached to a methyl group. The five states in $CHBr_2COCF_3^+$ correspond to either removing an electron from the oxygen lone pair or from the two lone pairs on each bromine.

The argument above requires the presence of Br for the existence of many ionic states with similar energies and, thus, one would not expect to find these states in an acetone without Br substituents. In order to demonstrate this, we performed similar calculations for the halogenated acetone CH_3COCF_3, for which we do not find any evidence of a charge transfer resonance at 1.5 eV during dissociation after ionization. Figure 4 shows the lowest-lying states of CH_3COCF_3 as a function of $C-CF_3$ bond length. There exists a much larger energy gap between the ground and first excited states as compared to $CHBr_2COCF_3^+$. In fact, the excited states are separated by at least 4 eV from the ground state at all $C-CF_3$ distances. The dashed line again indicates the initial energy of a wave packet (the energy of the ground state at the geometry of the neutral).

Unconstrained minimization at the CASSCF or MP2 level did not yield a minimum, implying that this cation is unstable. The very small barrier shown in Fig. 4 may be an artifact of the way the calculations were performed (optimized at the UHF level and then obtaining the energies at the higher MCQDPT2 level). Initial vertical ionization of CH_3COCF_3 is 0.93 eV above the minimum energy path to dissociation, so direct dissociation will occur more easily than in $CHBr_2COCF_3^+$. As in $CHBr_2COCF_3^+$, there are two dissociation channels in $CH_3COCF_3^+$: $CH_3CO^+ + CF_3$ and $CH_3CO + CF_3^+$. These channels are separated by 2.07 eV adiabatically (with all geometries of the fragments optimized) at the MP2/cc-pVDZ level of theory.

The calculations in $CH_3COCF_3^+$ are consistent with our earlier experimental results[15] that found a weak probe pulse (one capable of driving single-but not multiphoton resonances at 1.5 eV) produced no change in the fragment ion yields as a function of pump-probe delay. We found no single-photon resonances as the $C-CF_3$ bond dissociates.

The results in $CH_3COCF_3^+$ are consistent with Br being responsible for the low-energy cationic excited states and, consequently, charge transfer resonance in $CHBr_2COCF_3^+$. More generally, what appears to be important for the existence of low-energy, ionic excited states is the possibility of removing an electron from different orbitals with similar energies. For example, one should not expect low-energy ionic states in acetone. Indeed, the first and second ionization energies in acetone are separated by about 3 eV (9.71 and 12.59 eV, respectively),[16] in agreement with this argument. In a chloro-substituted acetone, an intermediate situation between $CH_3COCF_3^+$ and $CHBr_2COCF_3^+$ is expected since the IE in CH_3Cl is 11.3 eV (Ref. 17) between those of CH_3Br and CH_3F. One may extend these arguments even to different families of molecules, such as halogenated methanes if two or more similar type halogens are present, i.e., $CH_2IBr_2^+$.[6] The existence of a dynamic charge transfer resonance, of course, depends on the PES of the excited states and the different ionic PES must lead to different fragments in order to observe the charge transfer resonance in a TOFMS.

Finally, we comment on the existence of potential barriers in the ground ionic state when comparing the two acetones. One can understand the presence of a barrier by looking at the initial ion and the final fragments. Calculations show that initial ionization in CH_3COCF_3 creates an unpaired electron on oxygen. At the dissociation limit, $CF_3 + CHBr_2CO^+$, the unpaired electron has been moved to the CF_3 fragment, so this transfer has to occur during the dissociation and there will be a diabatic change of the ground cationic state. This change creates a barrier at the simplest level of theory. In $CHBr_2COCF_3$, our calculations show that initial ionization creates an unpaired electron on one of the Br atoms (the unpaired electron could have been on oxygen or either Br since they have similar ionization energies). Similar to CH_3COCF_3, at the dissociation limit the unpaired electron has moved to the CF_3 fragment, and a transfer must occur during dissociation creating a barrier. The two barriers present in $CHBr_2COCF_3$ could also be explained due to the hole occupying different fragments in this cation: the carbonylic oxygen, the bromine atoms in the $CHBr_2$ group, or the CF_3 group. We find that the character of the wave function changes as one moves out along the PES. Initially, the unpaired electron is on Br, after the first barrier it moves to oxygen, and finally to the CF_3 fragment. This complicated wave function behavior may explain why the barrier is so sensitive to the level of theory. If the wave function is not described correctly, it does not provide the correct barrier height. For example, a wave function that keeps the electron mainly on Br (a MCSCF using an active space with only bromine orbitals) creates an abnormally high barrier.

VII. CONCLUSION

By comparing high-level *ab initio* electronic structure calculations with time-resolved experimental measurements of dissociative ionization in $CHBr_2COCF_3$, we have developed a detailed picture of the fragmentation dynamics initiated by shaped and unshaped ultrafast laser pulses. We find that while the ground state of the ion has multiple barriers to dissociation, the initial wave packet launched via strong field ionization has sufficient energy to go over barriers along the $C-CF_3$ and $C-CHBr_2$ coordinates, producing the ionic fragments $CHBr_2^+$, $CHBr_2CO^+$, and CF_3^+. For dissociation along the $C-CF_3$ coordinate, the positive charge of the molecular ion is mostly localized on the acetyl ($CHBr_2CO$) fragment. However, the first excited state of the ion corresponds to a charge transfer state, with the positive charge mostly on the methyl (CF_3) fragment. Since the first excited state of the ion comes into resonance (1.5 eV separation) with the ground state as the dissociative wave packet moves out along the $C-CF_3$ coordinate, a probe pulse following the ionization pulse can promote the wave packet to the first excited state of the ion, leading to a depletion of the $CHBr_2CO^+$ and $CHBr_2^+$ yields and an enhancement of the CF_3^+ yield. In order to generalize our result, we interpret a comparison of the electronic spectra of two different molecular ions in terms of the ease with which one can move the unpaired electron left by ionization around the molecule.

ACKNOWLEDGMENTS

This research was supported by the National Science Foundation [T.W. (Award No. 0555214) and S.M. (Award No. CHE-0449853)] and the Research Corporation under award number R10956. K.G. was partially supported by the Louis Stokes Alliance for Minority Participation funded by the National Science Foundation.

[1] H. Harada, S. Shimizu, T. Yatsuhashi, S. Sakabe, Y. Izawa, and N. Nakashima, Chem. Phys. Lett. **342**, 563 (2001).
[2] L. Robson, K. W. D. Ledingham, A. D. Tasker, P. McKenna, T. McCanny, C. Kosmidis, D. A. Jaroszynski, D. R. Jones, R. C. Issac, and S. Jamieson, Chem. Phys. Lett. **360**, 382 (2002).
[3] H. Harada, M. Tanaka, M. Murakami, S. Shimizu, T. Yatsuhashi, N. Nakashima, S. Sakabe, Y. Izawa, S. Tojo, and T. Majima, J. Phys. Chem. A **107**, 6580 (2003).
[4] S. A. Trushin, W. Fuss, and W. E. Schmid, J. Phys. B **37**, 3987 (2004).
[5] D. Cardoza, B. J. Pearson, and T. Weinacht, J. Chem. Phys. **126**, 084308 (2007).
[6] B. J. Pearson, S. R. Nichols, and T. Weinacht, J. Chem. Phys. **127**, 131101 (2007).
[7] F. Langhojer, D. Cardoza, M. Baertschy, and T. Weinacht, J. Chem. Phys. **122**, 014102 (2005).
[8] T. H. Dunning, Jr., J. Chem. Phys. **90**, 1007 (1989).
[9] D. E. Woon and T. H. Dunning, Jr., J. Chem. Phys. **98**, 1358 (1993).
[10] P. J. Hay and W. R. Wadt, J. Chem. Phys. **82**, 270 (1985).
[11] M. W. Schmidt, K. K. Baldridge, J. A. Boatz, S. T. Elbert, M. S. Gordon, J. H. Jensen, S. Koseki, N. Matsunaga, K. A. Nguyen, S. Su, T. L. Windus, M. Dupuis, J. A. Montgomery, J. Comput. Chem. **14**, 1347 (1993).
[12] M. J. Frisch, G. W. Trucks, H. B. Schlegel *et al.*, GAUSSIAN 03, revision c.02, Gaussian, Inc., Wallingford, CT, 2004.
[13] D. Cardoza, B. J. Pearson, M. Baertschy, and T. Weinacht, J. Photochem. Photobiol., A **180**, 277 (2006).
[14] S. Anand, M. M. Zamari, G. Menkir, R. J. Levis, and H. B. Schlegel, J. Phys. Chem. A **108**, 3162 (2004).
[15] D. Cardoza, M. Baertschy, and T. Weinacht, J. Chem. Phys. **123**, 074315 (2005).
[16] V. Y. Young and K. L. Cheng, J. Chem. Phys. **65**, 3187 (1976).
[17] NIST Standard Reference Database No. 69 (http://webbook.nist.gov/chemistry/).